Journal of Science and Technology **54** (3A) (2016) 39-51

A NOVEL METHOD FOR DESIGNING THE CONTROLLER OF A LCL-FILTER-BASED GRID-CONNECTED INVERTER WITH CONSIDERING VARYING SYSTEM PARAMETERS

Nguyen Trung Nhan[1, *], Nguyen Thi Hanh[2]

[1]*Faculty of Electrical Engineering, Industrial University of Ho Chi Minh City, 12 Nguyen Van Bao St, Ward 4, Go Vap Dist, Ho Chi Minh City, Viet Nam*

[2]*Faculty of Information Technology, Industrial University of Ho Chi Minh City, 12 Nguyen Van Bao St, Ward 4, Go Vap Dist, Ho Chi Minh City, Viet Nam*

[*]Email: *nguyentrungnhan@iuh.edu.vn*

Received: 15 June 2015; Accepted for publication: 26 July 2016

ABSTRACT

Exactly determining the control coefficients for the controller of a three-phase LCL-filter-based inverter is an important and challenging issue in microgrid systems. However, existing LCL-filter-based inverter systems usually assume that all system parameters are determined accurately and remain constant over time, which is not true in real situations. Variations in the system parameters are known to possibly seriously degrade the performance of LCL-filter-based inverter systems. For efficiency and robustness, this paper proposes a novel method for the generalized controller design of a three-phase LCL-filter-based grid-connected inverter system that can address deviations in system parameters. An optimum way to determine the stability bounds under various system parameters cases is introduced. The assessment of the stability bounds is based on the Routh criterion by solving the characteristic equation of the closed-loop control system. Simulations results are presented to validate the correctness and effectiveness of the proposed design method.

Keywords: LCL filter, stability criterion, control quality, renewable energy resources.

1. INTRODUCTION

In recent years, penetration of renewable energy resources-based distributed generations (DGs) into the power grid is increasing worldwide at a significant rate. This is an inevitable development because of issues of fossil fuels, energy crisis, as well as environmental pollution and warming due to the greenhouse effect is becoming more and more serious, and it is concerned from countries in the world. As a result, renewable energy-based DGs have been rapidly developed. In distributed systems, the presence of DGs has formed a network of distributed generations and they are referred to as the microgid [1]. The high penetration of DGs in traditional power systems is one of the essential factors that could help to solve the energy crisis and improve power supply reliability. However, the involvement of DGs in the main grid

has caused problems, such as harmonic distortion and spinning reserve, especially in the stand-alone mode of the microgrid [2 - 3]. One of the most important approaches to address these problems is the improvement of control quality and the reliability of converters used in DGs systems. To this end, the voltage source inverter (VSI) is the most important module of the converters used in renewable-energy-based DGs [4]. The VSIs acts as a DC/AC converter, which convert a DC voltage to an AC voltage with the grid frequency in order to inject the active and reactive power to the main grid. To improve the injected-current and voltage quality of the VSI, a low-pass filter is required to filter out the harmonic elements. In general, L-, LC-, and LCL-filter are three types of filters that are commonly used to suppress the harmonic elements of the current injected into the main grid. In three types of filters, the LCL-filter has received much attention because it can improve the performance over other types of filters. However, the VSI incorporating LCL-filter is a three-order system. If the controller is inappropriately designed, the system may become unstable due to the resonant peak and the presence of zero impedance to the harmonics at the resonant frequency from the VSI or the main grid [5]. Many control strategies have been proposed to dampen the resonance, and they can be divided into two main strategies: active damping and passive damping. In [6], a passive resistor was added to the LCL-filter to dampen the resonance. This method is a simple to implement and often used for industrial applications. However, a major drawback of this method is the production of extra loss. To decrease the losses in passive damping, a new method for determining the optimized passive damping resistor of LCL and LLCL filters has been proposed in [7]. However, the losses persist here, which constitutes a significant challenge for widely using the VSI with an LCL-filter in practice.

Compared with the passive methods, the active damping methods are more commonly used to deal with the resonance due to the LCL-filter. In [8], a control method based on the virtual flux concept has been proposed. In this method, the capacitor currents are estimated from the capacitor voltage by a virtual flux model. Hence, this method can prevent phase lag and the distortion of the remaining high-frequency components. In [9], a resonance compensation method based on adding some compensation terms into the controller of the VSI in the PQR-frame has been proposed. In this method, the AC components of the input current are mitigated to reduce the harmonic components due to the resonance. Usually, a controller of the LCL-filter-based grid-connected inverter requires two feedback signals, the grid-side current and capacitor (or inverter-side) current. To decrease the number of sensors, a control strategy based on the splitting the capacitor of the LCL-filter was proposed in [10]. In this strategy, two capacitors are placed in parallel at the position of the capacitor in the LCL-filter, and the current between the two capacitors is measured as the feedback signal. In [11], the authors analyzed the generalized stability of a grid-connected VSI with an LCL-filter and proposed a control strategy to improve the transient and steady-state performance called composite nonlinear feedback. In [12-13], the authors analyzed and evaluated the applicability of each part of the overall control in a weak grid with the use of a stability criterion.

As outlined above, studies that aimed to improve the effectiveness and accuracy of the VSI with an LCL-filter have been implemented and have satisfied our expectations. In general, the controller of a VSI with an LCL-filters issued for fixed system parameters (i.e., the resistances, inductances, capacitors are constants). However, the responses of the control system depend on the system parameters in real control systems. The studies in [14-15] indicated that the stability and injected-current quality of DGs strongly depend on the system parameters. Unfortunately, these system parameters cannot be accurately determined because their values vary with the environment temperature, operating time, and equipment quality. Thus, the quality, stability, and

target of control systems will not be satisfied during operation. To address this issue, several control methods for DGs have been proposed based on LCL-filter by considering uncertain system parameters. A controller that could reject the uncertain parameters to eliminate the impact of the variation of main grid parameters was proposed in [16-17]. However, its implementation is difficult because its design requires an observation method and a convergence study. To improve the stability of the controller of the VSI with an LCL-filter based on increasing the bandwidth of the proportional-resonant controller, a new control method called weighted average current control was proposed in [18]. In this method, the feedback current is multiplied by an average factor that is determined from system parameters. In references [19 - 21], a method based on full-feed forward functions was proposed to improve the control quality and stability of the control system. In [22 - 23], a new method based on feedback the capacitor current with reduced computation delay for improving robustness of the controller of LCL filter-based grid-connected inverter was proposed. In [24 - 25], to mitigate the impact of the grid voltage disturbance and grid impedance change, a method based on direct grid current control was proposed. The studies in these papers have indicated that the stability and control quality directly relates to the number of feedback signals of the VSI with an LCL-filter controller if the control coefficients are reasonably designed. In these works, the variations of the system parameters are also mentioned in the design of controller. However, these papers do not provide a specific method to determine the precise control parameters. To bridge this gap, a robust controller design method used in VSI with an LCL-filter has been proposed in [26]. In these works, the coefficients of controller are designed based on the root-locus of the transfer function while considering the system parameter variation. However, the changes in the coefficients of controller and system parameters are considered independently of each other.

In this paper, a novel method for designing the controller of a three phase LCL-filter-based grid-connected inverter is proposed to bridge the aforementioned gaps. In the proposed method, the coefficients of the controller are generally determined based on the system parameters and the variation of these parameters. The proposed method guarantees the robustness and stability of the controller of the three-phase LCL-filter-based grid-connected inverter for the system performance, irrespective of the change in the system parameters.

The rest of the paper is organized as follows. The topology and mathematical model of the three-phase LCL-filter-based grid-connected inverter are presented in Section 2. In Section 3, the multi-loop controller for the three phase LCL filter-based grid-connected inverter is presented. Section 4 will analyze the change of control coefficient bounds versus the change of system parameters. The generalized controller design method and its implementation for improving the control quality of three phase LCL filter-based gird-connected inverter system are presented in Section 5. Section 6 shows the simulation results of the proposed method. Finally, the conclusion is presented in Section 7.

2. MATHEMATICAL MODEL OF THREE PHASE LCL-FILTER-BASED GRID-CONNECTED INVERTER

The general topology of the renewable-energy-based distributed generator used in the paper comprises a renewable energy resource, a DC-DC (AC-DC) converter, and a standard three-phase VSI connected to the main grid through an LCL-filter, as shown in Figure 1. Where, L_{1a}, L_{1b}, and L_{1c} are the inverter-side inductors, respectively; R_{1a}, R_{1b}, and R_{1c} are the internal resistances of the inductances L_{1a}, L_{1b}, and L_{1c}, respectively; R_{2a}, R_{2b}, and R_{2c} are the internal resistances of the grid-side inductances L_{2a}, L_{2b}, and L_{2c}, respectively; C_a, C_b, and C_c are the filter

capacitors. Kirchhoff's laws are applied to the Figure 1 as follows:

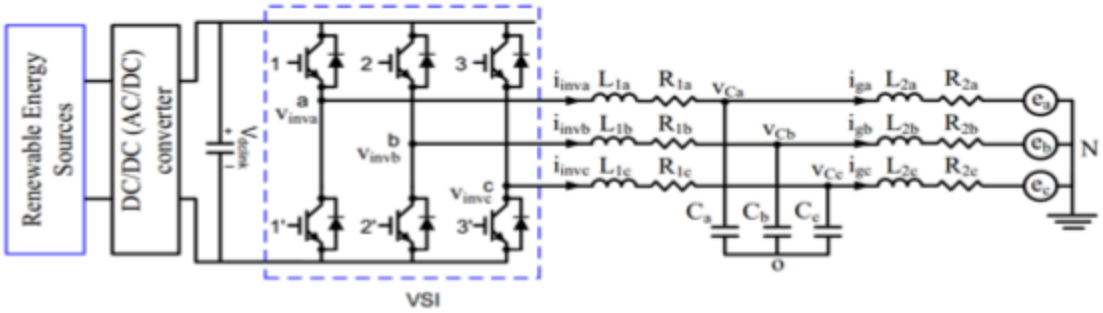

Figure 1. Topology of the three-phase LCL-filter-based grid-connected inverter.

$$v_{inv\xi} = v_{C\xi} + L_{1\xi}\frac{di_{inv\xi}}{dt} + R_{1\xi}i_{inv\xi} \tag{1}$$

$$v_{C\xi} = v_{g\xi} + L_{2\xi}\frac{di_{g\xi}}{dt} + R_{2\xi}i_{g\xi} \tag{2}$$

$$i_{inv\xi} = C_{\xi}\frac{dv_{C\xi}}{dt} + i_{g\xi} \tag{3}$$

Where, ξ={a,b,c}. The system parameters can be assumed that to be in balance without loss of generality (i.e., $L_{1\xi} = L_1$, $R_{1\xi} = R_1$; $L_{2\xi} = L_2$, $R_{2\xi} = R_2$; and $C_{\xi} = C$). No zero-sequence injected grid current was also assumed for the three-wire three-phase grid-connected inverter. Therefore, the state-space equations (1)-(3) can be written in the stationary α−β frame as follows:

$$\frac{di_{inv\alpha}}{dt} = -\frac{R_1}{L_1}i_{inv\alpha} + \frac{v_{C\alpha} - v_{g\alpha}}{L_1} \tag{4}$$

$$\frac{di_{inv\beta}}{dt} = -\frac{R_1}{L_1}i_{inv\beta} + \frac{v_{C\beta} - v_{g\beta}}{L_1} \tag{5}$$

$$\frac{di_{g\alpha}}{dt} = -\frac{R_2}{L_2}i_{g\alpha} + \frac{v_{g\alpha} - v_{C\alpha}}{L_2} \tag{6}$$

$$\frac{di_{g\beta}}{dt} = -\frac{R_2}{L_2}i_{g\beta} + \frac{v_{g\beta} - v_{C\beta}}{L_2} \tag{7}$$

$$i_{inv\alpha} = C\frac{dv_{C\alpha}}{dt} + i_{g\alpha} \tag{8}$$

$$i_{inv\beta} = C\frac{dv_{C\beta}}{dt} + i_{g\beta} \tag{9}$$

3. MULTI-LOOP CONTROLLER FOR LCL-FILTER-BASED GRID-CONNECTED INVERTER

As mentioned in Section 1, many methods have been proposed to address the controller design issue of the LCL-filter-based grid-connected inverter. To this end, the active damping based on multi-loop control is most commonly used because of its strong points. The multi-loop

control method proposed in [21] was adopted in this study. The control block of the three phase LCL-filter-based grid-connected inverter based on the multi-loop controller for the stationary α−β frame is shown in Figure 2. In this control block, the filter-capacitor current is used as the inner loop signal through a control gain (K_{c1}) and grid current tracked as the outer loop signal through a control gain (K_{c2}). Note that the control loops in this case act as full-feed forward functions [21]. In Figure 2, $G_c(s)$ is the main controller of the system. This controller might be a proportional-integral (PI) controller, a proportional resonant (PR) controller, harmonic compensation controller, or deadbeat controller. In this paper, a PI controller will be considered. $G_{inv}(s)$ is the transfer function of VSI. Normally, the switching frequency is much high than the fundamental frequency of the power grid. Therefore, with the three-phase pulse width modulator based on sine-triangle, the transfer function of VSI is a constant and can be approximately determined from the DC input voltage and the amplitude of the triangle carrier.

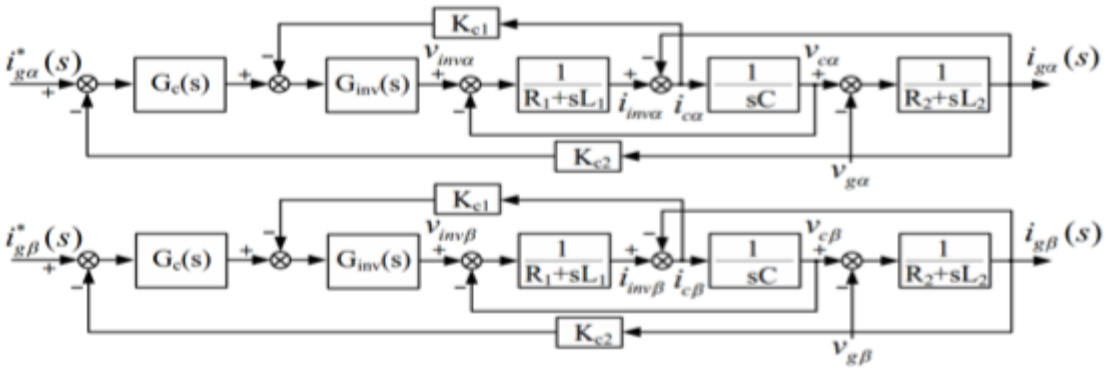

Figure 2. Control block of the three-phase LCL-filter-based grid-connected inverter in the stationary α−β frame.

In Figure 2, $i_{g\alpha}$ and $i_{g\beta}$ represents the output currents of the multi-loop controller; $i^*_{g\alpha}$ and $i^*_{g\beta}$ represents the reference currents in the stationary α−β frame. From Figure 2, the open-loop transfer function of the system is obtained as follows:

$$G_0(s) = \frac{G_c(s).G_i(s)}{H(s)} \tag{10}$$

where H(s) can be expressed in (11) as follows:

$$\begin{aligned} \mathrm{H(s)} &= \mathrm{L_1L_2Cs^3 + \{L_2CK_{c1}G_i(s) + R_1L_2C + L_1CR_2\}s^2 +} \\ &\quad \mathrm{+ \{L_1 + L_2 + R_2CK_{c1}G_i(s) + R_1R_2C\}s + (R_1 + R_2)} \end{aligned} \tag{11}$$

From (10), the closed-loop transfer function of the system is also obtained as follows:

$$G(s) = \frac{G_c(s).G_i(s)}{H(s) + K_{c2}.G_c(s).G_i(s)} \tag{12}$$

In this paper, the main controller is a PI controller formed as (13); therefore, the closed-loop transfer function (12) can be expressed in (14) as follows:

$$G_c(s) = K_p + \frac{K_i}{s} \tag{13}$$

$$G(s) = \frac{(K_p s + K_i).G_i(s)}{b_4 s^4 + b_3 s^3 + b_2 s^2 + b_1 s + b_0} \tag{14}$$

where, K_p, K_i are the proportional and integral gains of the PI controller, respectively. The coefficients of the polynomial denominator in (14) were determined as follows:

$$\begin{cases} b_4 = L_1L_2C;\ b_3 = L_2CK_{c1}G_i(s) + R_1L_2C + L_1CR_2 \\ b_2 = L_1 + L_2 + CR_2K_{c1}G_i(s) + R_1R_2C;\ b_1 = R_1 + R_2 + K_pG_i(s);\ b_0 = (K_{c2} + K_i)G_i(s) \end{cases} \quad (15)$$

Normally, the root locus method is a very common technique used to determine the control coefficients. In this technique, the root locus is plotted as a function of one of the coefficients while all of the other coefficients are fixed. This process is undertaken for all of the control coefficients, and the bounds of coefficients are determined. However, in the multi-loop control system, the integral gain (K_i) and the inner-loop control gain (K_{c1}) would not strongly affect the system stability (not strongly affect the location of the dominated poles), and they are often determined according to the steady-state error requirement. Contrary to the K_i and K_{c1}, the changes in the proportional gain (K_p) and outer-loop control gain (K_{c2}) significantly affect the system stability. Specifically, the proportional gain (K_p) affects not only the system stability but also the steady-state error [27-28]. Therefore, the selection of suitable K_p and K_{c2} values is a very important problem in multi-loop control system design.

4. ANALYSIS OF THE CHANGE OF CONTROL COEFFICIENT BOUNDS VERSUS THE CHANGE OF SYSTEM PARAMETERS

The quality of the control system depends on control coefficients which can change according to the system parameters. Hence, the changes in the system parameters are well known to be able to seriously degrade the performance and robustness of a VSI with LCL-filter systems. However, system parameters are not constants in real-world situations; they may change over time due to environmental conditions, operating times, the quality of equipment, etc., and may not be accurately determined. This drawback may prevent high quality control and stability in real operations. In this section, we analyze the dependence of the system performance on the system parameters. To validate the change of the system performance on the system parameters, we created a random data set that includes 98 subsets of the system parameters, respectively. In this study, we assumed that the change in system parameters is limited to ± 50% of the initial values (*i.e.*, $0.5\{R_{i0}, L_{i0}, C_0\} \leq \{R_{ik}, L_{ik}, C_k\} \leq 1.5\{R_{i0}, L_{i0}, C_0\}$), where i = {1, 2}; R_{i0}, L_{i0}, and C_0 are the initial values of the system parameters, as shown in Table 1; R_{ik}, L_{ik}, and C_k are the values of the system parameters at the k^{th} random point (rp).

Table 1. Parameters of the system.

AC grid line-line voltage	V_s = 380 V(rms)
AC grid frequency	f = 50 Hz
Inverter-side impedance	L_1 = 5.5 mH, R_1 = 0.2 Ω
Grid-side impedance	L_2 = 3.5 mH, R_2 = 0.2 Ω
Filter capacitance	C = 20 μF
$G_i(s)$	40
Switching frequency	10 kHz
V_{dc}	400 (V)

Table 2. The change of dominated **poles** (DPs) versus the change of system parameters.

rp	DPs	rp	DPs	rp	DPs	rp	DPs	rp	DPs	rp	DPs	rp	DPs
1	-31.550±5511i	15	**56.920±4546i**	29	**121.62±5350i**	43	**39.110±3904i**	57	**43.040±4700i**	71	-14.840±4075i	85	-520.62±5964i
2	-443.00±6400i	16	-278.81±6741i	30	**32.920±4526i**	44	-159.64±4773i	58	**25.960±3840i**	72	-319.35±5335i	86	-287.25±4697i
3	**58.080±5661i**	17	-64.040±5856i	31	**66.190±7459i**	45	-111.50±5991i	59	-43.530±3763i	73	**77.900±4458i**	87	**7.1700±4703i**
4	**44.690±6142i**	18	-16.070±3968i	32	-443.47±4118i	46	-197.60±4026i	60	-143.16±5683i	74	**42.010±4128i**	88	-217.74±4721i
5	**75.780±5049i**	19	**32.380±4527i**	33	-86.450±4998i	47	-330.51±4876i	61	-1.7300±4694i	75	**6.8600±5255i**	89	-26.930±5156i
6	-151.58±5346i	20	-329.26±7022i	34	**118.44±6632i**	48	**83.520±6258i**	62	**6.0400±3769i**	76	**119.57±6661i**	90	**24.360±5075i**
7	-170.17±4960i	21	**33.480±3767i**	35	-298.96±6224i	49	-136.57±5704i	63	**31.240±3968i**	77	**44.570±4477i**	91	-410.52±5267i
8	-210.46±5259i	22	**46.070±6170i**	36	**45.830±6525i**	50	-38.920±4265i	64	-247.08±3949i	78	-6.8700±4749i	92	-355.79±5457i
9	-44.010±6166i	23	**103.72±4683i**	37	-565.20±4232i	51	**3.0300±5866i**	65	-47.750±4015i	79	-258.44±3804i	93	-51.840±7653i
10	**114.69±4998i**	24	-594.16±5022i	38	-20.190±3662i	52	-318.27±5077i	66	-132.90±4031i	80	-373.03±4209i	94	-3.5300±5905i
11	-65.970±4742i	25	**69.830±5072i**	39	-95.470±5159i	53	**102.82±5902i**	67	-126.30±4287i	81	**100.69±5435i**	95	-55.570±4547i
12	-77.850±5225i	26	-295.38±6391i	40	-333.51±4487i	54	-318.10±5952i	68	-51.330±4285i	82	-1.0800±3594i	96	-395.12±4963i
13	**9.3700±6309i**	27	-53.900±4018i	41	-116.45±4569i	55	-194.08±4303i	69	-128.43±5085i	83	-356.74±4815i	97	-246.25±5255i
14	-92.120±4340i	28	-15.420±3923i	42	-26.100±4558i	56	**2.0500±4929i**	70	-49.770±5292i	84	-256.26±6289i	98	-43.180±5833i

The assessment is based on the *Routh* criterion by solving the characteristic equation of the closed-loop control system. The characteristic equation of the controller system is the closed-loop transfer function denominator polynomial of the system. According to the *Routh* criterion, a system is stable if and only if all of the roots of the characteristic equation have negative real parts (*i.e.*, all of the roots are in the left-half of the complex-plane). Based on this criterion, we determined the value of the dominated points (DPs) for each value of the system parameters by resolving the characteristic equation of the closed-loop control system. The change of DPs versus the change of system parameters obtained for this case (the value of K_p is determined for the initial values of the system parameters based on the root locus method) is shown in Table 2. This Table shows that have many cases of the DPs values unsatisfied the stability condition (**bolded text**) based on the *Routh* criterion. This means that the stability of the control system of the LCL-filter-based grid-connected inverter strongly depend on the system parameters.

5. GENERALIZED DESIGN METHOD FOR THE CONTROLLER OF LCL-FILTER-BASED GRID-CONNECTED INVERTER

As outline above, the controller gain obtained by using existing methods may not guarantee stability when system parameters change. As a result, the exact determination of the stability bounds when the system parameters change is extremely important and should be carefully carried out. In this paper, we propose a generalized design method for designing the controller of the three phase LCL-filter-based grid-connected inverter. In proposed method, we determine the optimal stability bound of the coefficient control gains for each value of the system parameters (this value called the local optimal stability bounds) by resolving the characteristic equation of the closed-loop control system. After determining these local optimal stability bounds, the global optimal coefficient control gains of the controller are determined based on the minimum (or maximum) rules. The proposed algorithm can be used to determine the stability bound of all control coefficient gains. However, as mentioned above, we only focused on the global optimal value of the proportional gain (K_p) in this paper. Hence, the global optimal proportional gain of

the controller is determined as follows:

$$K_{p-opt} = \min\{K_{p-opt-1}, K_{p-opt-2}, ..., K_{p-opt-n}\} \quad (16)$$

The proposed algorithm was coded in Matlab/M-file and used to obtain the random distribution of the local optimal stability bounds, which are shown in Table 3. This Table show that the stability bounds significantly depend on the system parameters. The global optimal value represents the range for the controller gain K_p that guarantees the stability irrespective of the change in system parameters, whereas the local optimal value represents the range for the controller gain that only guarantee stability for fixed system parameters.

Table 3. The change of local optimal stability bounds of the controller versus the change of system parameters.

rp	K_{p_Lopt}	rp	K_{p_Lopt}	rp	K_{p_Lopt}	rp	K_{p_Lopt}	rp	K_{p_Lopt}	rp	K_{p_Lopt}	rp	K_{p_Lopt}
1	2.1	15	1.9	29	1.7	43	1.9	57	1.9	71	2.1	85	3.3
2	3.0	16	2.7	30	2.0	44	2.5	58	2.0	72	2.7	86	2.7
3	1.9	17	2.2	31	1.9	45	2.3	59	2.2	73	1.8	87	2.0
4	1.9	18	2.1	32	3.2	46	2.6	60	2.4	74	1.9	88	2.6
5	1.8	19	2.0	33	2.2	47	2.8	61	2.1	75	2.0	89	2.1
6	2.4	20	2.6	34	1.8	48	1.8	62	2.0	76	1.8	90	2.0
7	2.4	21	1.9	35	2.7	49	2.4	63	2.0	77	1.9	91	2.9
8	2.5	22	1.9	36	2.0	50	2.2	64	2.8	78	2.1	92	2.9
9	2.2	23	1.8	37	3.4	51	2.0	65	2.2	79	2.8	93	2.1
10	1.8	24	3.4	38	2.1	52	2.8	66	2.4	80	3.0	94	2.1
11	2.3	25	1.9	39	2.3	53	1.8	67	2.3	81	1.8	95	2.2
12	2.3	26	2.8	40	2.8	54	2.8	68	2.2	82	2.1	96	2.9
13	2.0	27	2.2	41	2.3	55	2.5	69	2.4	83	2.8	97	2.6
14	2.3	28	2.1	42	2.1	56	2.0	70	2.2	84	2.6	98	2.1

Table 4. The change of dominated poles versus the change of system parameters if the value of K_p is accurately determined.

rp	DPs	rp	DPs	rp	DPs	rp	DPs	rp	DPs	rp	DPs	rp	DPs
1	-221.39±5447i	15	-86.600±4500i	29	-29.840±5306i	43	-87.530±3862i	57	-129.52±4633i	71	-167.92±4017i	85	-717.06±5924i
2	-655.25±6350i	16	-465.44±6702i	30	-126.69±4468i	44	-325.10±4723i	58	-110.17±3790i	72	-556.23±5243i	86	-510.40±4599i
3	-73.360±5632i	17	-249.99±5802i	31	-156.06±7392i	45	-330.17±5917i	59	-171.35±3722i	73	-71.630±4405i	87	-139.50±4658i
4	-94.140±6112i	18	-135.05±3934i	32	-639.42±4048i	46	-361.95±3968i	60	-295.16±5650i	74	-108.89±4071i	88	-390.86±4669i
5	-66.180±5009i	19	-139.58±4458i	33	-304.14±4901i	47	-541.35±4801i	61	-164.68±4639i	75	-200.60±5169i	89	-177.59±5115i
6	-325.13±5298i	20	-591.83±6939i	34	-78.570±6572i	48	-68.360±6221i	62	-127.58±3721i	76	-57.630±6613i	90	-124.51±5033i
7	-374.91±4881i	21	-91.300±3725i	35	-503.92±6170i	49	-328.57±5646i	63	-100.00±3924i	77	-116.37±4418i	91	-641.94±5185i
8	-413.40±5190i	22	-92.110±6141i	36	-163.79±6457i	50	-194.10±4211i	64	-408.39±3896i	78	-125.79±4722i	92	-534.30±5415i
9	-205.55±6127i	23	-52.180±4628i	37	-792.75±4141i	51	-170.85±5817i	65	-170.82±3981i	79	-418.99±3749i	93	-327.65±7556i
10	-75.170±4919i	24	-817.28±4957i	38	-154.36±3614i	52	-505.62±5025i	66	-284.97±3980i	80	-559.49±4145i	94	-134.24±5879i
11	-195.88±4710i	25	-87.920±5022i	39	-240.55±5124i	53	-56.400±5859i	67	-320.73±4198i	81	-62.840±5384i	95	-226.25±4486i
12	-205.89±5198i	26	-462.57±6359i	40	-567.08±4373i	54	-508.79±5906i	68	-192.98±4241i	82	-126.41±3550i	96	-625.27±4874i
13	-154.45±6270i	27	-185.66±3979i	41	-312.80±4485i	55	-371.58±4238i	69	-300.62±5034i	83	-582.99±4724i	97	-441.18±5195i
14	-253.06±4286i	28	-164.04±3867i	42	-197.77±4493i	56	-123.500±4899	70	-219.39±5241i	84	-456.78±6238i	98	-256.40±5757i

These Tables also show that the global optimal value is relatively near compared with local optimal value and unstable value. Note that the value of K_p can generally be chosen in the range of the global optimal area (namely, $K_p \leq K_{p\text{-}opt}$). However, in practice, the steady-state error of the control system will increase if the value of K_p decreases. Therefore, the best value of K_p is the value of $K_{p\text{-}opt}$ determined in (16). To test the correctness of the proposed algorithm, we used the global optimal value of K_p obtained from Table 3 and (16) to obtain the random distribution of the dominated poles when system parameters changes, which are shown in Table 4. This Table shows that the proposed algorithm is correctness.

6. SIMULATION RESULTS

The proposed design method for the three-phase LCL filter-based grid-connected inverter control system based on the *Routh* criterion was verified using a simulation in the Matlab/Simulink environment. The main purpose of the simulation was to test the effectiveness and correctness of the proposed method for designing controller used in the three-phase VSI with an LCL-filter when the system parameters are variable. In this simulation, the main frequency of the power grid is 50 Hz, the power grid voltage in this simulation is 380 V (phase-phase), and the control signal of the IGBTs is generated using a pulse-width modulation generator whose amplitude and frequency of the carrier wave are ± 10V and 10000Hz, respectively. The system parameters used in the simulations are given in Table 1. The value of K_p was assigned equal to the global stability bound (in this study $K_{p\text{-}opt}$ = 1.3). Figure 3 illustrates the grid voltage, the controller output currents ($i_{g\alpha}$, $i_{g\beta}$) in the stationary $\alpha-\beta$ frame, and the grid-side current in three-phase for a demand reactive power equal to zero (*i.e.*, the power factor equal to unit).

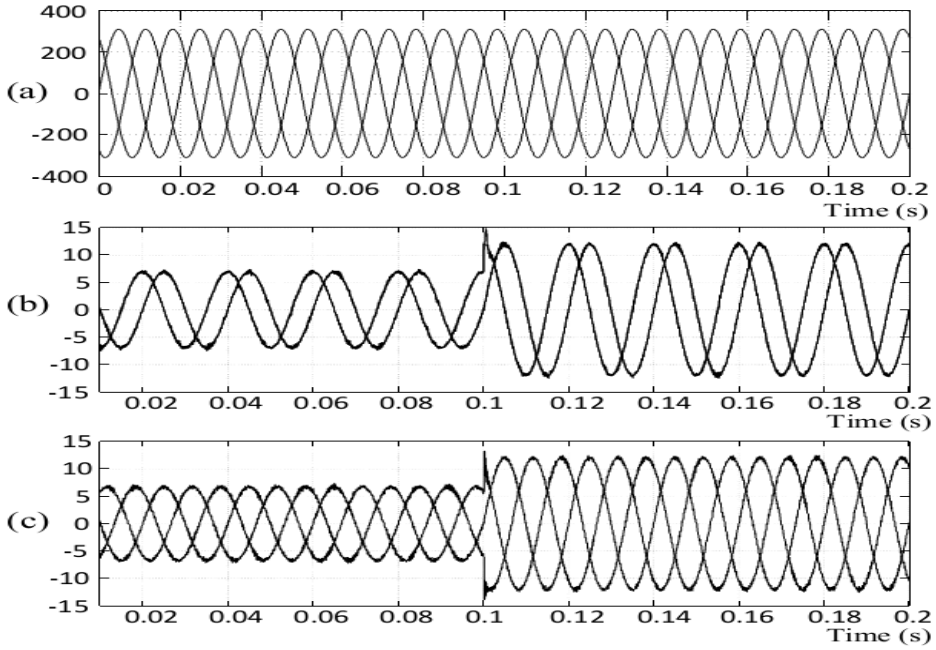

Figure 3. Simulation results of the proposed multi-closed-loop control system. (a) Grid voltages. (b) The controller output currents (i_α, i_β) in the stationary α−β frame. (c) The grid side current (i_g).

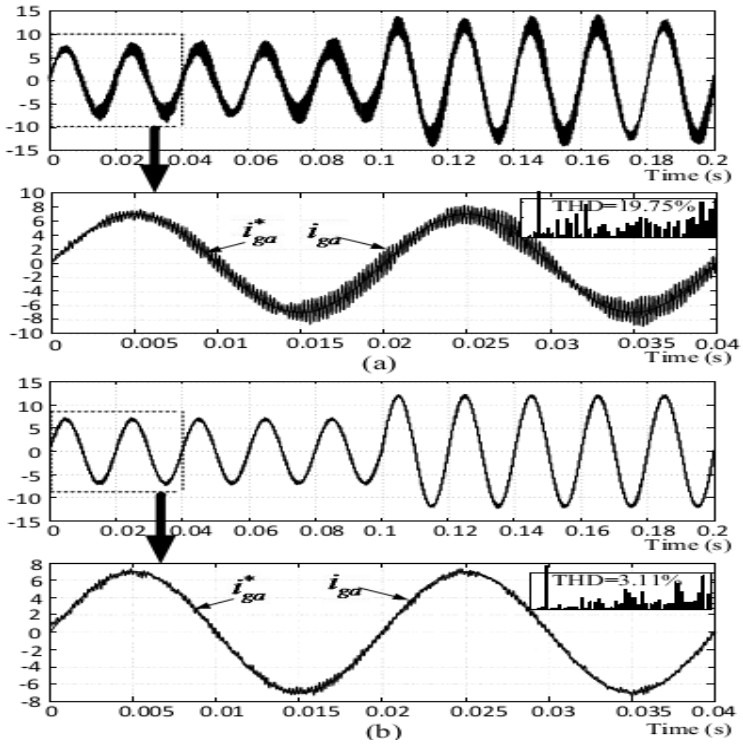

Figure 4. Simulation results when the system parameters changed. (a) K_p determined by conventional method. (b) K_p determined by proposed method.

To test the dynamic response of the proposed control system, the reference current was changed from 7 ampere to 12 ampere (peak) at $t = 0.1$ *s* when the system is operating (note that the change occurs when the a-phase current arrives at the zero value). This Figure shows that the dynamic response of the proposed controller is rapid for this case. Moreover, the steady-state error of the proposed controller is also very small. To verify the system performance is sensitive to the controller coefficients, simulations were performed when the system parameters changed (in this case: $C = 0.9C_0$, $L_1 = 0.9L_{10}$, $L_2 = 0.85L_{20}$, $R_1 = 0.8R_{10}$, and $R_2 = 0.8R_{20}$, as shown in Table 1) for two cases: the value of K_p was assigned equal to the initial stability bound (the value of K_p is determined for the initial values of the system parameters based on the root locus method) and the value of K_p was assigned equal to the global optimal stability bound (as detailed in Section 5), respectively. The simulation result for this case is shown in Figure 4. This Figure shows that the proposed design method guarantees the controller of the LCL filter-based grid-connected inverter robust operation, irrespective of the change in the system parameters while the conventional method is not. This finding demonstrates that the system performance is sensitive to the controller coefficients and can yield a good performance with the conventional PI controller if the controller coefficients are exactly designed. To verify the effectiveness and correctness of the proposed method for designing the controller, simulations were performed in which the value of K_p was assigned to exceed the stability bound. The simulation result for this case is shown in Figure 5, which shows that the system is not stable.

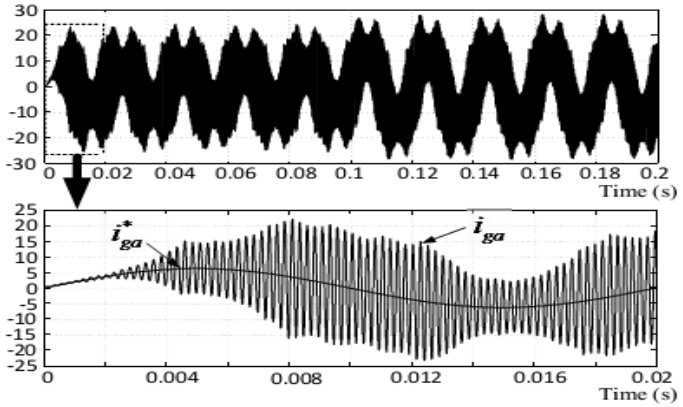

Figure 5. Simulation results for a value of K_p was assigned to exceed the stability bound.

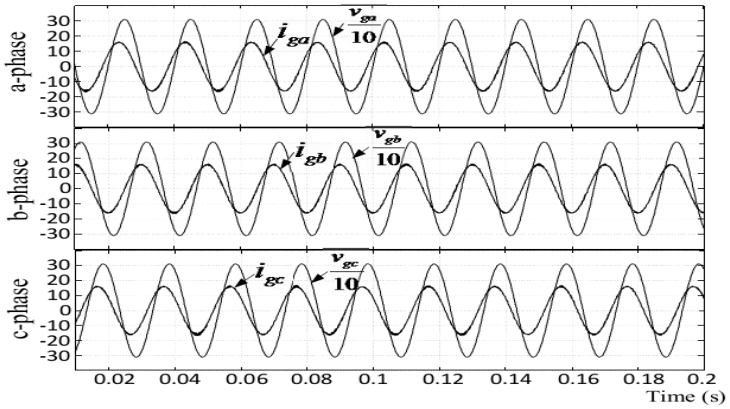

Figure 6. Simulation results for the power factor was 0.8 leading (with $K_p = K_{p\text{-}max\text{-}opt}$).

We now consider an REG operated in P-Q mode, namely, simultaneously injecting active and reactive power into the utility grid. The power factor was 0.8 leading. The simulation result for this case is shown in Figure 6. This Figure shows that the control system designed by using the proposed method resulted in efficiency and robust operation modes for all cases.

7. CONCLUSION

This paper proposes a generalized method to design the controller of a three phase LCL filter-based grid-connected inverter system. This design results in efficiency and robust operation for both fixed and variable system parameters. The impact of the change in system parameters on the performance of three phase LCL filter-based grid-connected inverter system was analyzed in detail. The proposed design method results in the correct operation of the controller of the three phase VSI with an LCL-filter system for fixed and variable parameters. Implementing the proposed design method using the solution of the equation based on conventional *Routh* criteria is simple. The analysis results in this paper demonstrate that the system performance is sensitive to the controller coefficients and can yield a good performance with conventional controllers if the controller coefficients are exactly determined. The simulation results show that the proposed method outperforms existing methods.

REFERENCES

1. Liserre A. T. M., Teodorescu R., Rodriguez P., Blaabjerg F. - Evaluation of current controllers for distributed power generation systems, IEEE T Power Electr. **24** (2009) 654-664.
2. Safigianni A. S., Koutroumpezis G. N., Poulios V. C. - Mixed distributed generation technologies in a medium voltage network, Electr. Power Syst. Res. **96** (2013) 75-80.
3. Pandi V. R., Zeineldin H. H., Wei X. D., Zobaa A. F. - Optimal penetration levels for inverter-based distributed generation considering harmonic limits, Electr. Power Syst. Res. **97** (2013) 68-75.
4. Nguyen T. N., Luo A. - Multifunction converter based on Lyapunov function used in a photovoltaic system. Turk J. Elec. & Comp. Sci. **22** (2014) 893-908.
5. Liu Q., Peng L., Kang Y., Tang S., Wu D., Qi Y. - A novel design and optimization method of an LCL filter for a shunt active power filter, IEEE T. Ind. Electr. **61** (2014) 4000-4010.
6. Figueres E., Gabriel G., Sandia G. J., Gonzalez-Espin F., Rubio J. C. - Sensitivity study of the dynamics of three-phase photovoltaic inverters with an LCL grid filter, IEEE T. Ind. Electr. **56** (2009) 706-717.
7. Wu W., He Y., Tang T., Blaabjerg F. - A new design method for the passive damped LCL and LLCL filter-based single-phase grid-tied inverter, IEEE T. Ind. Electr. **60** (2013) 4339-4350.
8. Gullvik W., Norum L., Nilsen R. - Active damping of resonance oscillations in LCL-filters based on virtual flux and virtual resistor, Proc. EPE (2007) 1–10.
9. Jeong H. G., Lee K. B., Choi S., Choi W. - Performance improvement of LCL-filter-based grid-connected inverters using PQR power transformation, IEEE T. Power Electr. **25** (2010) 1320-1330.
10. Shen G., Xu D., Cao L., Zhu X. - An improved control strategy for grid-connected voltage source inverters with an LCL filter, IEEE T. Power Electr. **23** (2008) 1899-1906.
11. Eren S., Pahlevaninezhad M., Bakhshai A., Jain P. K. - Composite nonlinear feedback control and stability analysis of a grid-connected voltage source inverter with LCL filter, IEEE T. Ind. Electr. **60** (2013) 5059 - 5074.
12. Xu J., Xie S., Tang T. - Evaluations of current control in weak grid case for grid-connected LCL-filtered inverter, IET Power Electr. **6** (2013) 227-234.
13. Mariethoz S., Morari M. - Explicit model-predictive control of a PWM inverter with an LCL filter, IEEE T. Ind. Electr. **56** (2009) 389-399.
14. Bahrani B., Vasiladiotis M., Rufer A. - High-order vector control of grid-connected voltage-source converters with LCL-filters, IEEE T. Ind. Electr. **61** (2014) 2767-2775.
15. Nguyen T. N., Luo A. - A generalized design method for multifunction converter used in photovoltaic system, Turk J. Elec. Eng. & Comp. Sci. **24** (2016) 882-895.
16. Mohamed Y. A. R. I. - Suppression of low and high-frequency instabilities and grid-induced disturbances in distributed generation inverters, IEEE T. Power Electr. **26** (2011) 3790-3803.

17. Hao X., Yang X., Liu T., Huang L., Chen W. - A sliding-mode controller with multiresonant sliding surface for single-phase grid-connected VSI with an LCL filter, IEEE T. Power Electr. **28** (2013) 2259-2268.
18. He N., Xu D. H., Zhu Y., Zhang J., Shen G. Q., Zhang Y. F., Ma J., Liu C. J. - Weighted average current control in a three-phase grid inverter with an LCL filter, IEEE T. Power Electr. **28** (2013) 2785-2797.
19. Wang X., Ruan X., Liu S., Tse C. K. - Full feedforward of grid voltage for grid-connected inverter with LCL filter to suppress current distortion due to grid voltage harmonics, IEEE T. Power Electr. **25** (2010) 3119-3127.
20. Xue M., Zhang Y., Kang Y., Yi Y., Li S., Liu F. - Full feedforward of grid voltage for discrete state feedback controlled grid-connected inverter with LCL filter, IEEE T. Power Electr. **27** (2012) 4234-4247.
21. Li W., Ruan X., Pan D., Wang X. - Full-feedforward schemes of grid voltages for a three-phase LCL-type grid-connected inverter, IEEE T. Ind. Electr. **60** (2013) 2237-2250.
22. Pan D., Ruan X., Bao C., Li W., Wang X. - Capacitor-Current-Feedback active damping with reduced computation delay for improving robustness of LCL-type grid-connected inverter, IEEE T. Power Electr. **29** (2014) 3414-3427.
23. Bao C., Ruan X., Wang X., Li W., Pan D., Weng K. - Step-by-step controller design for LCL-type grid-connected inverter with capacitor–current-feedback active-damping, IEEE T. Power Electr. **29** (2014) 1239-1253.
24. Jia Y., Zhao J., Fu X. - Direct grid current control of LCL-filtered crid-connected inverter mitigating grid voltage disturbance, IEEE T. Power Electr. **29** (2014) 1532-1541.
25. Xu J., Xie S., Tang T. - Active damping-based control for grid-connected LCL-filtered inverter with injected grid current feedback only, IEEE T. Ind. Electr. **61** (2014) 4746-4758.
26. Li B., Yao W., Hang L., Tolbert L. M. - Robust proportional resonant regulator for grid-connected voltage source inverter (VSI) using direct pole placement design method, IET Power Electr. **5** (2012) 1367-1373.
27. Pena-Alzola R., Liserre M., Blaabjerg F., Sebastian R., Dannehl J., Fuchs F. W. - Systematic design of the lead-lag network method for cctive damping in LCL-filter based three phase converters, IEEE T. Ind. Inform. **10** (2014) 43-52.
28. Nguyen T. N., Luo A., Shuai Z. K., Chau M. T., Li M. F., Zhou L. M. - Generalised design method for improving control quality of hybrid active power filter with injection circuit, IET Power Electronic **7** (2014) 1204-1215.